JOURNAL OF CATALYSIS 70, 111–122 (1981)

# Isomerization of Cyclopropane on Synthetic Faujasite by Pulse Technique

## II. Experimental Study

M. A. SCHOBERT AND Y. H. MA

*Department of Chemical Engineering, Worcester Polytechnic Institute, Worcester, Massachusetts 01609*

Received October 13, 1980; revised January 26, 1981

The parameters for sorption, intercrystalline and intracrystalline diffusion, and reaction were determined for the isomerization of cyclopropane to propylene over synthetic faujasite ($Li^{ex}Y$, NaY, and $K^{ex}Y$). The parameters were obtained from studying the response of a continuous stirred tank reactor (CSTR) containing catalyst powder or pellets, when an impulse of cyclopropane is introduced in the reactor. The model developed for the CSTR was used successfully for the determination of the parameters for diffusion, adsorption, and chemical reaction. Both micro- and macroeffectiveness factors were obtained and the results indicated that the intracrystalline diffusion was rate limiting and that the intracrystalline diffusion coefficients were lowered by the presence of a reaction. Also it was found that $K^{ex}Y$ was inactive for the isomerization of cyclopropane over the temperature range considered.

## INTRODUCTION

The need for a better understanding of the relative importance of the phenomena such as adsorption, diffusion, and reaction involved in a catalytic system is well recognized. However, it is rather difficult to study these phenomena simultaneously, especially when catalysts such as zeolites involving both inter- and intracrystalline diffusion are considered. Wheeler (*1*) and Satterfield (*2*) have studied the coupling of mass transfer and chemical reaction extensively and have given a number of references on the subject. Most of the work has been done using gas chromatographic techniques and considered cases where one or two processes were insignificant. Intensive work on the subject was done by Smith and co-workers (*3–11*). However, in gas chromatographic techniques, axial dispersion and external mass transfer have to be taken into account. This generally complicates the mathematical treatment of the problem. The literature shows that a standard continuous stirred tank reactor (CSTR) (*12–14*) as well as specially designed reactors like the single-pellet reactor of Balder and Petersen (*15, 16*) may be used to investigate kinetics and diffusional effects in catalytic operation. It is particularly useful to conduct the experiments in a CSTR since external heat and mass transfer rates are greatly enhanced. Another important consideration when modeling catalytic systems is the choice of a well-known system. This is the case for the isomerization of cyclopropane which was studied thermally first, by Chambers and Kistiakowsky (*17*) and Schlag and Rabinovitch (*18*). The reaction was also studied on acidic solids like platinum, alumina, and platinum supported on alumina by Roberts (*19*). Hall and co-workers (*20–23*) investigated the isomerization reaction over a silica–alumina catalyst. Habgood and co-workers (*24–26*) used a gas chromatographic pulse technique to study the reaction over X and Y zeolite catalysts. In all cases it was found that the reaction was an irreversible first-order reaction. However, diffusion in zeolites was not considered in these studies and only intrinsic rates of reaction were determined. In a novel approach, Kelly (*27*) studied the cy-



0021-9517/81/070111-12$02.00/0

clopropane isomerization over a slab catalyst of NaX zeolite, using a CSTR and including diffusion and adsorption. However, his model does not apply to spherical pellets which are commonly used as catalysts.

The objective of this work is to determine the parameters of adsorption, inter- and intracrystalline diffusion, and first-order reaction using a CSTR. The parameters are obtained from the description of the transient behavior of the CSTR when a concentration impulse of reactant is introduced. The results then provide information about the rate-controlling step in a catalyst having a biporous distribution.

## EXPERIMENTAL TECHNIQUE

The continuous stirred tank catalytic reactor consisted of a cylindrical stainless-steel vessel of $2.38 \times 10^{-3}$-$m^{-3}$ capacity and was employed to study sorption, diffusion, and reaction of cyclopropane isomerization over Y zeolites. The powder (microporous crystals dispersed in glass wool) or the spherical pellets (with a biporous distribution) were placed in two equally spaced adjustable baskets which were attached to the shaft and were rotated during the experiments. The design is essentially similar to that of Carberry (*28*). The shaft was driven by a $\frac{1}{12}$-hp motor at a constant speed. A schematic diagram of the apparatus is shown in Fig. 1. Heating was done by three heating rods (G) placed inside stainless-steel castings (1.5 cm in diameter) to avoid possible contamination or sorption of gas by the heating elements. The stainless-steel castings also served as baffles to facilitate mixing. The temperature of the system was controlled by a West controller (I) within $\pm 0.5$°C.

Residence time distribution done by a tracer technique on a similar system (*29*) showed that the system was essentially well mixed. Experiments performed with different rotation speeds and calculations (*30*) showed that external mass transfer was negligible.

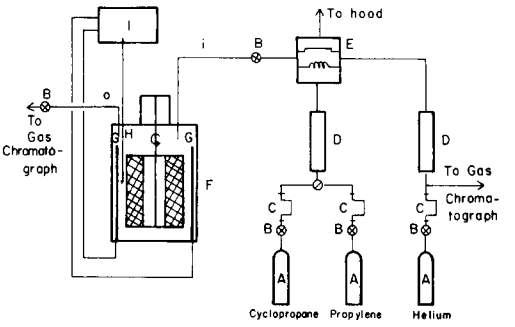


FIG. 1. Schematic diagram of the CSTR apparatus. A, gas cylinder; B, stopcock; C, moisture trap; D, rotameter; E, injection valve; F, constant-volume reactor; G, heating rod; H, thermocouple; I, temperature controller; i, gas inlet; o, gas outlet.

Helium was used as a carrier gas and the flow was adjusted at the inlet of the reactor by a rotameter (D) and measured at the outlet of the reactor with a bubble flowmeter. The inlet of the reactor was fitted with an injection valve equipped with a 10-$cm^3$ loop (E). Samples of the exiting gas were introduced through a second injection valve into the gas chromatograph for analysis. The Perkin–Elmer 900 gas chromatograph was equipped with a flame ionization detector and a CSI-2000 digital integrator. A Porapak N column of 0.318 cm diameter and 1.83 m length was used. The column temperature was 160°C and the carrier flow rate was 30 $cm^3$/minute.

The starting material was NaY zeolite powder and was obtained from Linde division, Union Carbide Corporation (Lot No. 96805000). $K^{ex}Y$ and $Li^{ex}Y$ zeolites were prepared by contacting the initial NaY zeolite with potassium chloride and lithium and determined by X-ray fluorescence chemical analysis to be 97% for the K form and 59% for the Li form. As shown by X-ray diffraction patterns, the crystal structure was not affected by the ion exchange. The individual crystals in the powder varied slightly in size. A cross section of 500 crystals was observed under the electron microscope and the average radius was found to be equal to 25 $\mu$m. As for the pellets used in the experiments, they were made by mixing

TABLE 1

Composition of Zeolites

| | $Li^{ex}Y$ | NaY | $K^{ex}Y$ |
|---|---|---|---|
| $SiO_2$, wt% | 69.46 | 67. | 62.58 |
| $Al_2O_3$, wt% | 21.46 | 20.55 | 19.44 |
| $Na_2O$, wt% | 5.33 | 11.83 | 0.29 |
| $K_2O$, wt% | 0 | 0 | 18.60 |
| $Li_2O$, wt% | 3.75 | 0 | 0 |
| Si/Al molar ratio | 2.74 | 2.77 | 2.73 |
| Percentage exchange | 59.4 | 0 | 97.4 |

85% (by weight) of zeolite powder to 15% of kaolin binder (Georgia Kaolin Company). The spherical pellets thus formed were screened and only beads with size between mesh 4 and 5 (average diameter 4.32 mm) and between mesh 5 and 6 (average diameter 3.36 mm) were used in the experiments. The macroporosity was determined by mercury porosimetry and the microporosity was obtained from the zeolite structure (*30*). The characteristics of the material (powder and pellets) are shown in Tables 1 and 2.

For each run, zeolite was placed in the baskets. Each basket contained approximately 1.5 g of the zeolite. The zeolite was then activated for about 6 h under helium atmosphere at 370°C and cooled to the desired temperature. The motor was then started and the baskets were rotated in the reactor at 3600 rpm. When the temperature was stabilized the flow rate of helium was adjusted to the chosen flow rate, and cyclopropane was flowed through the injection loop. At time $t = 0$, cyclopropane was injected into the reactor through the injection valve and the concentration of cyclopropane was sampled at the exit of the reactor with the gas chromatograph. Sampling was continued until the exit concentration of the reactant and product gases approached zero. A digital integrator was used to calculate the area under the chromatographic peak and the gas concentration $Y$. Once the curve $Y$ versus $t$ (exit concentration versus time) was obtained, the data were fed to the computer. A program was used to fit the experimental curve to a polynomial expression and to calculate $\mu_0$, $\mu_1$, and $\mu_2$ (the zeroth-, first-, and second-order moments of the curve). As described in the preceding paper, the values of $I$, $I'$, and $I''$ and $J$, $J'$, $J''$ are derived from the moments and are employed to evaluate the micro- and macroeffectiveness factors $\eta_i$ and $\eta_a$, and the modified micro- and macro-Thiele moduli $\phi_i$ and $\phi'_a$. This then leads to the determination of the adsorption equilibrium constant $K_a$, the reaction rate constant $k_s$, the intracrystalline diffusivity $D_i$, and the intercrystalline diffusivity $D_a$.

## RESULTS AND DISCUSSIONS

Experiments were performed with $Li^{ex}Y$, NaY, and $K^{ex}Y$ zeolites, using both powder and pellets. At least three different flow rates were used for each sample and for each of the three temperature settings (225, 250, and 275°C). Typical response curves to an impulse are shown in Fig. 2. The data were then processed according to the procedure described in the preceding paper to obtain the parameters for sorption, diffusion, and reaction. It should be noted that no reaction could be observed with $K^{ex}Y$ zeolite between 225 and 275°C.

### *Adsorption Equilibrium Constant $K_a$*

The modified micro-Thiele modulus $\phi_i$ can be obtained by combining the characteristic functions $I$, $I'$, and $I''$ for powder

TABLE 2

Characteristics of Material

| Material | Density ($kg/m^3$) | Porosity | Radius of particle (m) | Surface area ($m^2/g$) |
|---|---|---|---|---|
| $Li^{ex}Y$ powder | 1786. | 0.48 | $2.545 \times 10^{-7}$ | 539.56 |
| NaY powder | 1899. | 0.48 | $2.545 \times 10^{-7}$ | 517.48 |
| $K^{ex}Y$ powder | 1915. | 0.48 | $2.545 \times 10^{-7}$ | 518.95 |
| $Li^{ex}Y$ pellet | 1120. | 0.385 | $0.216 \times 10^{-2}$ | 443.15 |
| NaY pellet | 1143. | 0.479 | $0.217 \times 10^{-2}$ | 441.88 |
| $K^{ex}Y$ pellet | 1173. | 0.484 | $0.212 \times 10^{-2}$ | 458.17 |

(*30*) according to

$$\frac{I''(I-1)}{(I'-\tau)^2} = \frac{(\phi_i \cosh \phi_i - \sinh \phi_i)(2\phi_i \cosh \phi_i - \phi_i \sinh \phi_i - \cosh \phi_i \sinh^2 \phi_i)}{\phi_i(\cosh \phi_i \sinh \phi_i - \phi_i)^2}. \quad (1)$$

The parameter $K_a$ can then easily be obtained from the slope of the line representing $I'$ versus $1/F$ since

$$I' = \frac{V}{F} + \frac{3}{2}\frac{\nu_i}{F}\epsilon_i(1 + K_a)M(\phi_i). \quad (2)$$

$M(\phi_i)$ is a hyperbolic function of $\phi_i$ as given in Eq. (28) in the preceding paper and takes a given value for each sample.

In the case of no reaction ($k_s = 0$) Eq. (2) reduces to the normalized first-order moment

$$I' = \bar{\mu}_1 = \frac{V}{F} + \frac{\nu_i}{F}\epsilon_i(1 + K_a). \quad (3)$$

A similar expression is obtained for pellets:

$$J' = \bar{\mu}_1 = \frac{V}{F} + \frac{\nu_a}{F}\epsilon_a + \tau_a\epsilon_i(1 - \epsilon_a)(1 + K_a). \quad (4)$$

The results for the adsorption equilibrium constant, obtained from experiments with powder are shown in Table 3. A comparison between these values and those determined in previous experiments (*30*) using a Cahn electromagnetic microbalance can be made. The agreement is certainly quite reasonable considering the fact that the extrapolation of the Cahn balance data was done over a large temperature range (45 to 275°C). These results appear to substantiate the validity of the model.

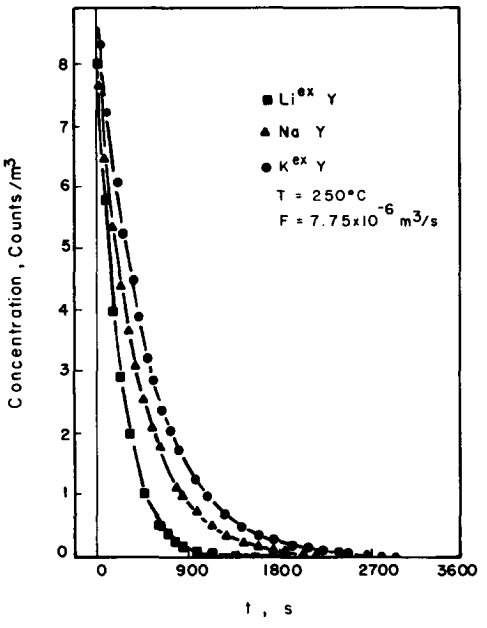


FIG. 2. Response curve of CSTR at 250°C for $Li^{ex}Y$, NaY, and $K^{ex}Y$ powder.

In the case of no reaction ($K^{ex}Y$ zeolite), $K_a$ was also obtained with pellets. As shown in Table 3, the $K_a$ values obtained for $K^{ex}Y$ pellets are slightly lower than the $K_a$ values obtained with $K^{ex}Y$ powder. This discrepancy may be attributed to the presence of the inert binder in the pellets. In fact, an excellent agreement is obtained if the inert weight is considered in the calculation (less than 6% difference).

The isosteric heat of adsorption was obtained from a semilog plot of the adsorption equilibrium constant, $K_a$ versus $1/T$ according to the Van't Hoff equation. The results for all three zeolites are plotted in Fig. 3 which shows that straight lines are obtained for all three cases. This indicates that the isosteric heat of adsorption is constant over the temperature range considered. The values of the isosteric heat of adsorption thus obtained are shown in Table 3 and are slightly higher than those obtained with a Cahn electromagnetic microbalance (*30*). However, they agree within 10% and follow the same increasing order:

$$\Delta H_{K^{ex}Y} < \Delta H_{NaY} < \Delta H_{Li^{ex}Y}.$$

The highest heat of adsorption is obtained with $Li^{ex}Y$ (smaller cation) due in part, to the larger electrical field created by Li cation in the zeolite structure. Therefore, the interaction between the adsorbate and

TABLE 3

Variations of $K_a$ with Temperature and Heat of Adsorption for $Li^{ex}Y$, NaY, and $K^{ex}Y$ Zeolites

| Sample | Temperature (°C) | $K_a$ determined from Cahn balance | $K_a$ determined with CSTR and powder | $K_a$ determined with CSTR and pellets | $\Delta H_a$ isosteric heat of adsorption (kJ/mol) |
|---|---|---|---|---|---|
| $Li^{ex}Y$ | 225 | 605 | 481 | | |
| | 250 | 384 | 291 | | 43.5 |
| | 275 | 255 | 185 | | |
| NaY | 225 | 575 | 448 | | |
| | 250 | 378 | 280 | | 39.0 |
| | 275 | 298 | 190 | | |
| $K^{ex}Y$ | 225 | 515 | 426 | 384 | |
| | 250 | 345 | 271 | 245 | 38.9 |
| | 275 | 240 | 181 | 163 | |

the zeolite is greater for $Li^{ex}Y$ than that for NaY or $K^{ex}Y$.

*Reaction Rate Constant*

Once the parameter $\phi_i$ is known, the microeffectiveness factor $\eta_i$ can be evaluated from

$$\eta_i = \frac{3}{\phi_i^2}(\phi_i \coth \phi_i - 1). \quad (5)$$

Since $K_a$ has already been determined, the reaction rate constant $k_s$ may be obtained from the slope of the straight line by plotting $I$ versus $1/F$ according to

$$I = 1 + \frac{\nu_1}{F}\epsilon_i K_a k_s \eta_i. \quad (6)$$

The experiments showed that $K^{ex}Y$ did not have any catalytic activity for the isomerization of cyclopropane between 225 and 275°C, whereas NaY was moderately active and $Li^{ex}Y$ quite active.

The numerical values for the reaction rate constant for $Li^{ex}Y$ and NaY are summarized in Table 4 along with the energies of activation. The energy of activation was obtained from the semilog plot of $k_s$ versus $1/T$, according to the Arrhenius-type equation:

$$k_s = k_{s0} \exp(-E_a/RT). \quad (7)$$

The Arrhenius plot is shown in Fig. 4 and the excellent straight lines obtained indicate that the energies of activation are constant over the temperature range investigated. Furthermore, the values obtained here are in good agreement with those

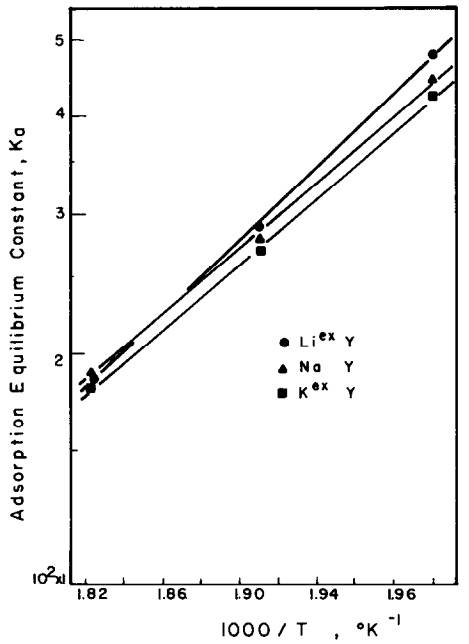


FIG. 3. Semilog plot of adsorption equilibrium constant as a function of $1/T$ for cyclopropane on $Li^{ex}Y$, NaY, and $K^{ex}Y$ powder.

TABLE 4

Variations of $k_s$ with Temperature for $Li^{ex}Y$ and NaY Powder

| Sample | Temp (°C) | $k_s$ ($s^{-1}$) | $E_a$ (kJ/mol) |
|---|---|---|---|
| $Li^{ex}Y$ | 225 | $1.65 \times 10^{-2}$ | |
| | 250 | $3.70 \times 10^{-2}$ | 69.9 |
| | 275 | $7.71 \times 10^{-2}$ | |
| NaY | 225 | $4.89 \times 10^{-4}$ | |
| | 250 | $1.51 \times 10^{-3}$ | 98.4 |
| | 275 | $4.26 \times 10^{-3}$ | |

obtained by other investigators. Chambers and Kistiakowsky (*17*) and Schlag and Rabinovitch (*18*) reported an energy of activation of about 272 kJ/mol. However, this was for the thermal isomerization of cyclopropane and the values are much lower when catalysts are used. For example, Roberts (*19*) reported an energy of activation of 79.5 kJ/mol on a silica–zirconia–alumina catalyst while Hall *et al.* (*22*) reported a value of 71.2 kJ/mol on a silica–alumina catalyst. Finally, Basset and Habgood (*25*) reported a value of 125.6 kJ/mol with a 13X zeolite, and $3.8 \times 10^{-3}$ $s^{-1}$ for the rate constant $k_s$ at 250°C. Their heat of adsorption of 46.1 kJ/mol is also in good agreement with the values indicated earlier. The study of Habgood and George (*26*) on the isomerization of cyclopropane on X and Y zeolites, lead them to the conclusion that the activity increased in the order KX < NaX < NaY < LiX < HY, between 160 and 370°C. They indicated that the rate constants $k_s$ are one or two orders of magnitude larger for Y zeolites than for X zeolites. Also, they reported values for the rate constant at 250°C equal to $1.8 \times 10^{-5}$ $s^{-1}$ for NaX and $2.8 \times 10^{-3}$ $s^{-1}$ for LiX. The values of $k_s$ obtained with the CSTR method are, therefore, in good agreement with those reported by Habgood and George. As for the activation energy on NaY, the value of 98.4 kJ/mol compares well with the 103 kJ/mol given by Habgood and George. It was reported by the same authors that the activation energy for LiY was lower but no experimental value was reported. The value of 69.9 kJ/mol obtained here appears very reasonable.

These results on the reaction rate constant show that the catalytic activity varies significantly with the cation. Such variations were reported by other researchers (*26*). The cyclopropane isomerization is an acid-catalyzed reaction and probably proceeds through Brønsted sites. Since the activity is strongly dependent on the nature of the exchangeable cation, the number and maybe the strength of the Brønsted sites are probably directly related to the cation. Also, since adsorption properties are only slightly affected by the exchangeable cation, it seems that adsorption sites and catalytic sites may be different or that not all adsorption sites are catalytically active.

### *Intracrystalline Diffusion Coefficients $D_i$*

The intracrystalline diffusion coefficient may be obtained from the modified micro-

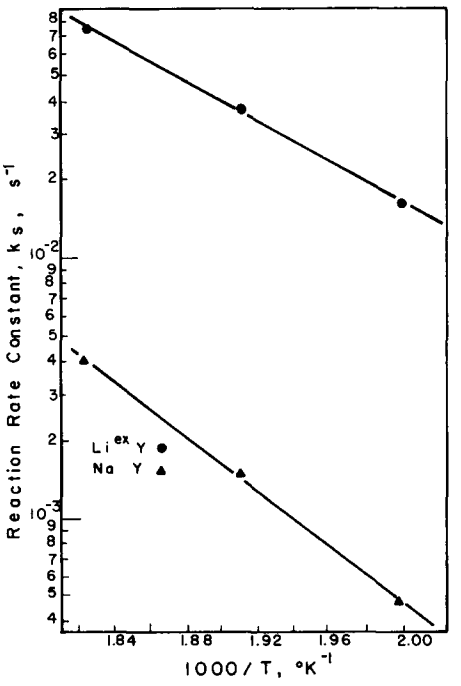


FIG. 4. Arrhenius plot of reaction rate constant for cyclopropane on $Li^{ex}Y$ and NaY powder.

Thiele modulus $\phi_i$ using

$$D_i = \frac{R_i^2 k_s K_a}{\phi_i^2}. \quad (8)$$

The numerical values of $D_i$ are shown in Table 5. Values obtained by extrapolation of previous measurements (*30*) with a Cahn electromagnetic microbalance are also indicated for comparison. The values for $K^{ex}Y$ are in close agreement for both methods (within 3%) which shows that the model describes well the diffusion and sorption processes. However, in the presence of a reaction (as for $Li^{ex}Y$ and NaY), the diffusion coefficients determined from the CSTR experiments are lower by about 26% for $Li^{ex}Y$ and 16% for NaY. These results seem to indicate that the diffusional process is affected by the presence of a chemical reaction. The slowing down of the diffusional process may be due to the counter-diffusion of the reaction product which prevents the reactant from diffusing freely in the pores. However, it may be argued that the reduction of the diffusion coefficient attributed to the presence of a reaction may be unlikely, especially with an isomerization reaction. This reduction may, therefore, be due to the effects of other phenomena not taken into account in the modeling. For example, the adsorption step may not be at equilibrium and the adsorption of product species may not be negligible. The lumping of these parameters may then cause a variation on the effective diffusion coefficient. It was also found that the reaction rate obtained for $Li^{ex}Y$ is higher than that for NaY. This is consistent with the higher reduction in diffusion coefficient obtained with $Li^{ex}Y$.

TABLE 5

Variations of $D_i$ with Temperature for $Li^{ex}Y$, NaY, and $K^{ex}Y$ Powder

| Sample | Temp (°C) | $D_i \times 10^{-15}$ (m²/s) | Activation energy (kJ/mol) |
|---|---|---|---|
| $Li^{ex}Y$ | 225 | 2.19 (2.99)[a] | |
| | 250 | 2.65 (3.57)[a] | 16.75 (15.49)[a] |
| | 275 | 3.16 (4.20)[a] | |
| NaY | 225 | 1.49 (1.75)[a] | |
| | 250 | 1.71 (1.99)[a] | 9.63 (10.89)[a] |
| | 275 | 1.84 (2.23)[a] | |
| $K^{ex}Y$ | 225 | 1.41 (1.38)[a] | |
| | 250 | 1.55 (1.52)[a] | 8.79 (8.37)[a] |
| | 275 | 1.71 (1.66)[a] | |

[a] Obtained from measurements with the Cahn balance.

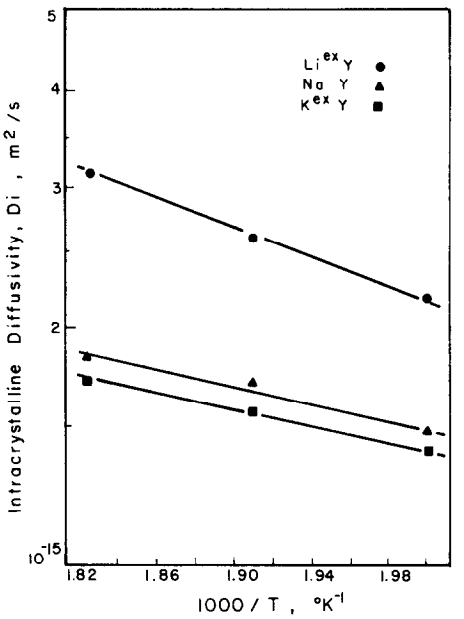


FIG. 5. Arrhenius plot of intracrystalline diffusivity for cyclopropane on $Li^{ex}Y$, NaY, and $K^{ex}Y$ powder.

The activation energies for intracrystalline diffusion were determined from the Arrhenius-type equation:

$$D_i = D_{i0} \exp(-E_i/RT). \quad (9)$$

A semilog plot of $D_i$ versus $1/T$ for $Li^{ex}Y$, NaY, and $K^{ex}Y$ powder is given in Fig. 5. The linearity is very good in all cases, indicating that the energies of activation are constant over the temperature range investigated. As can be seen in Table 5, the CSTR values are very close (within 7%) to the values obtained in previous experiments (*30*) with a Cahn balance. The intracrystalline diffusion coefficient decreases in the following order:

$$D_{i_{Li^{ex}Y}} > D_{i_{NaY}} > D_{i_{K^{ex}Y}}.$$

As in the case of the heat of adsorption, the order of increasing energy of activation for diffusion may be related to the increase of electrostatic field created by the cation in the zeolite.

*Intercrystalline Diffusion Coefficient $D_a$*

One additional parameter has to be determined when using pellets: the intercrystalline diffusion coefficient $D_a$. A plot of the characteristic function $J$ versus $1/F$ gives a straight line whose slope may be used to calculate $\eta_a$ as indicated by

$$J = 1 + \frac{\nu_a}{F} \epsilon_i(1 - \epsilon_a)K_a k_s \eta_i \eta_a \quad (10)$$

with

$$\eta_a = \frac{3}{\phi_a'^2} (\phi_a' \coth \phi_a' - 1) \quad (11)$$

and

$$\phi_a' = \left[\frac{R_a^2 K_a k_s}{D_a} \frac{\epsilon_i(1 - \epsilon_a)}{\epsilon_a} \eta_i\right]^{1/2} \quad (12)$$

$D_a$ can then be determined by solving Eq. (11) for $\phi_a'$ and Eq. (12) for $D_a$.

The results are shown in Table 6 which also lists diffusion coefficients obtained from the kinetic theory of gases for comparison. According to the kinetic theory of gases, the mean free path of cyclopropane in the temperature range between 225 and 275°C and under atmospheric pressure is approximately 800 Å. Since mercury porosimeter measurements gave an average macropore diameter of 1100 Å, the Knudsen number is 0.73 (800/1100). Thus, the diffusion in the macropore is expected to be in the transition regime and the diffusion coefficient can be estimated from the Bosanquet formula (*31*).

$$\frac{1}{D_t} = \frac{1}{D_k} + \frac{1}{D_{C,H}}. \quad (13)$$

The intracrystalline diffusion coefficient $D_a$ was compared to the transition regime diffusion coefficient to obtain the tortuosity factor $\gamma$, as defined by

$$\gamma = D_t/D_a. \quad (14)$$

Table 6 gives the diffusion coefficients for bulk diffusion $D_{C,H}$, Knudsen diffusion $D_k$, transition regime diffusion $D_t$, intercrystalline diffusion $D_a$ as well as the tortuosity factor $\gamma$. The tortuosity factor varies between 3.9 and 4.6 but the values are relatively constant for each type of zeolite and no temperature dependence is observed. The average value of 4.2 is very reasonable since values between 2 and 7 are commonly reported for similar material. The slight variations in tortuosity factor may be attributed to differences in pellet porosity and density. However, the fact that the tortuos-

TABLE 6

Diffusion Coefficients for Knudsen, Bulk, and Transition Regime, Intercrystalline Diffusion Coefficient, and Tortuosity Factor

| Sample | Temp (°C) | $10^6 \times D_k$ (m²/s) | $10^6 \times D_{C,H}$ (m²/s) | $10^6 \times D_t$ (m²/s) | $10^6 \times D_a$ (m²/s) | $\gamma = D_t/D_a$ |
|---|---|---|---|---|---|---|
| $Li^{ex}Y$ | 225 | 19.5 | 107.3 | 16.5 | 3.57 | 4.61 |
| | 250 | 19.9 | 116.2 | 17.0 | 3.83 | 4.44 |
| | 275 | 20.4 | 125.3 | 17.5 | 3.89 | 4.51 |
| NaY | 225 | 19.5 | 107.3 | 16.5 | 3.84 | 4.28 |
| | 250 | 19.9 | 116.2 | 17.0 | 3.89 | 4.37 |
| | 275 | 20.4 | 125.3 | 17.5 | 4.05 | 4.34 |
| $K^{ex}Y$ | 225 | 19.5 | 107.3 | 16.5 | 4.11 | 4.00 |
| | 250 | 19.9 | 116.2 | 17.0 | 4.35 | 3.92 |
| | 275 | 20.4 | 125.3 | 17.5 | 4.51 | 3.89 |

ity factor is relatively constant appears to further substantiate the validity of the model.

*Contribution of the Diffusional Resistances*

As indicated previously, zeolite pellets exhibit a bipore distribution which generates two types of diffusional processes:

—a zeolitic diffusion in the well-defined micropores (9 Å in diameter for Y zeolite) of the individual crystals.

—a transition regime diffusion in the macropores (about 0.1 $\mu$m in diameter for this study) formed when crystals are bound together.

It is of prime importance to know the relative contribution of both diffusional processes and this subject has been studied by various investigators. Antonson and Dranoff (*32*) (for the sorption of ethane on 5A zeolite) and Roberts and York (*33*) (for the sorption of liquid *n*-paraffins on 5A zeolites) showed that both intercrystalline and intracrystalline diffusion played an important role. However, Sargent and Whitford (*34*) found that only intracrystalline diffusion was significant for $CO_2$ and 5A zeolites, especially at low temperatures. The studies of Youngquist *et al.* (*35*) and Mancel (*36*) for hydrocarbons on different zeolites, indicate that there are systems where intercrystalline diffusion is important. Mancel (*36*) also showed that his chromatographic method was able to determine the relative contribution of the intercrystalline and intracrystalline diffusion resistances to the overall resistance in a bed of zeolite pellets. The CSTR method presented here can also be used to determine the relative importance of each diffusional process (*30*). The contribution of the intercrystalline diffusion resistance and the intracrystalline diffusion resistance relative to the overall diffusional resistance was obtained for $K^{ex}Y$ and is shown in Table 7. It is evident that the intracrystalline diffusion resistance is much more important (more than 96%) than the intercrystalline diffusion resistance and is rate controlling. Some important results are also obtained in the presence of the isomerization reaction. In that case, the relative importance of diffusion to the overall rate process is determined from the effectiveness factor. Table 8 lists the modified micro- and macro-Thiele moduli and the micro- and macroeffectiveness factors and their products.

TABLE 7

Percentage Contribution of the Individual Diffusion Resistances to the Total Diffusion Resistance in Pellets

| Temperature (°C) | Intracrystalline diffusion resistance (%) | Intercrystalline diffusion resistance (%) |
|---|---|---|
| 225 | 96.70 | 3.30 |
| 250 | 96.43 | 3.57 |
| 275 | 96.16 | 3.84 |

TABLE 8

Values of Modified Thiele Moduli and Effectiveness Factors for $Li^{ex}Y$ and NaY

| Material | $T$ (°C) | $\phi_i$ | $\eta_i$ | $\phi'_a$ | $\eta_a$ | $\eta_i\eta_a$ |
|---|---|---|---|---|---|---|
| $Li^{ex}Y$ | 225 | 15.41 | 0.182 | 1.230 | 0.912 | 0.166 |
| | 250 | 16.26 | 0.173 | 1.346 | 0.897 | 0.155 |
| | 275 | 17.01 | 0.166 | 1.451 | 0.883 | 0.147 |
| NaY | 225 | 3.09 | 0.661 | 0.303 | 0.994 | 0.656 |
| | 250 | 4.02 | 0.561 | 0.386 | 0.990 | 0.556 |
| | 275 | 5.35 | 0.456 | 0.472 | 0.985 | 0.449 |

For both $Li^{ex}Y$ and NaY, the macroeffectiveness factor $\eta_a$ is close to 1, which indicates that intercrystalline diffusion is negligible as expected. The small values of the microeffectiveness factor $\eta_i$ show that the overall process is controlled by intracrystalline diffusion. It can be noted that $\eta_i$ decreases as temperature increases. This is to be expected since the activation energy for a chemical reaction is normally much higher than that of diffusion (e.g., $E_a$ = 69.9 kJ/mol and $E_i$ = 16.75 kJ/mol for $Li^{ex}Y$). It

is also interesting to note that $\eta_i$ is much smaller for $Li^{ex}Y$ than for NaY. This again is consistent with the fact that $Li^{ex}Y$ is more active than NaY. The same conclusion is reached from the observation of the overall effectiveness factor ($\eta_i\eta_a$).

These results appear to indicate that the method can be used successfully to estimate quantitatively the relative contribution of the interparticle and intraparticle diffusion resistances to the overall diffusion resistance. Moreover, it allows one to determine the rate-controlling step in a process involving reaction, adsorption, and diffusion phenomena.

## CONCLUSIONS

The determination of sorption, diffusion, and reaction rate parameters from the measurements of the response curves to concentration impulses applied to a CSTR, appears to be a promising method. The CSTR method was applied to the isomerization of cyclopropane over three different zeolites and gave values for the adsorption constant and the diffusion coefficients which were in close agreement with those obtained through other methods. (Cahn electromagnetic microbalance).

A general practice in determining the relative importance of diffusional resistances in a reacting system is to assume that the diffusion coefficient measured under the no reaction condition may be applied to a reacting system. Although the validity of such an assumption is generally uncertain, very little experimental evidence is currently available to substantiate this doubt. The present results appear to indicate that the diffusional processes may be somewhat affected by the presence of a chemical reaction. This results in the lowering of the diffusion coefficients and may give erroneous conclusions on the determination of the rate-controlling step. It should be pointed out that the relatively small reduction in the diffusion coefficient may be the result of low reactant concentration and that higher concentration may produce a larger reduction in the diffusion coefficient. However, it should be cautioned that the reduction in the diffusion coefficients may also be due to the effect of lumping the parameters not included in the modeling and analysis of the system. The CSTR method allows one to determine the relative importance of intercrystalline and intracrystalline diffusion coefficients to the overall diffusion resistance. Since micro- and macroeffectiveness factors are also determined, one can determine the rate-controlling step in a process involving diffusion, reaction, and adsorption. Although further development of the method may be needed, it appears to be very promising for evaluating sorption, intercrystalline, and intracrystalline diffusion parameters under reacting and nonreacting conditions. Care should be taken when using the method for a particular system and the assumptions of adequate mixing in the reactor and high mass transfer rates between the bulk phase and the catalyst should be thoroughly checked.

Interesting observations were made concerning the properties of zeolites related to the exchangeable cation. Although the sorption and diffusion properties vary from one zeolite to another, the differences are relatively small compared to the differences in reactivity. This may be attributed to the fact that the adsorption sites and active sites for reaction are of different natures. Also, the size of the cation is not the determining factor in diffusion and sorption properties. Rather, it is the electrostatic field created by the cations in the zeolite structure which has a predominant effect. It was also shown that the intercrystalline diffusion resistance is negligible in the overall diffusion resistance but that intracrystalline diffusion is the rate-controlling step for $Li^{ex}Y$ and NaY zeolites.

## APPENDIX: NOMENCLATURE

| | |
|---|---|
| $D$ | diffusion coefficient, $m^2/s$ |
| $D_{C,H}$ | diffusion coefficient of cyclopropane (C) in helium (H), $m^2/s$ |

$D_k$ Knudsen diffusion coefficient, $m^2/s$
$D_t$ diffusion coefficient for transition regime, $m^2/s$
$E$ activation energy, kJ/mol or kcal/mol
$F$ flow rate, $m^3/s$
$I$ characteristic function for crystals, evaluated at $S = 0$, dimensionless
$I'$ first derivative of characteristic function for crystals evaluated at $S = 0$, s
$I''$ second derivative of characteristic function for crystals evaluated at $S = 0$, $s^2$
$J$ characteristic function for pellets evaluated at $S = 0$, dimensionless
$J'$ first derivative of characteristic function for pellets evaluated at $S = 0$, s
$J''$ second derivative of characteristic function for pellets evaluated $S = 0$, $s^2$
$K_a$ equilibrium constant for adsorption, dimensionless
$k_s$ first-order surface reaction rate constant, $s^{-1}$
$R_a$ radius of pellet, m
$R_i$ radius of crystal, m
$t$ time, s
$T$ absolute temperature, K
$v$ volume of catalyst, $m^3$
$V$ volume of reactor, $m^3$

*Greek Letters*

$\gamma$ tortuosity
$\epsilon$ void volume = porosity, $m^3$ pore volume/$m^3$ pellet volume
$\mu$ moment
$\phi$ modified Thiele modulus for crystal, dimensionless
$\phi'$ modified Thiele modulus for pellet, dimensionless
$\eta$ effectiveness factor
$\tau = V/F$ residence time, s

*Subscripts*

i intracrystalline or micropore or powder
a intercrystalline or macropore or pellet
s surface

*Superscripts*

- normalized (moment)
^ central normalized (moment)

REFERENCES


1. Wheeler, A., *in* "Advances in Catalysis and Related Subjects," Vol. 3, p. 249. Academic Press, New York/London, 1951.
2. Satterfield, C. N., "Mass Transfer in Heterogeneous Catalysis." MIT Press, Cambridge, Mass., 1970.
3. Cerro, R. L., and Smith, J. M., *Ind. Eng. Chem. Fundam.* **8**, 796 (1969).
4. Cerro, R. L., and Smith, J. M., *AIChE J.* **16**, 1014 (1970).
5. Masamune, Sh., and Smith, J. M., *AIChE J.* **10**, 246 (1964).
6. Masamune, Sh., and Smith, J. M., *Ind. Eng. Chem. Fundam.* **3**, 179 (1964).
7. Masumune, Sh., and Smith, J. M., *AIChE J.* **11**, 34 and 41 (1965).
8. Padberg, G., and Smith, J. M., *J. Catal.* **12**, 172 (1968).
9. Schneider, P., and Smith, J. M., *AIChE J.* **14**, 762 (1968).
10. Schneider, P., and Smith, J. M., *AIChE J.* **14**, 886 (1968).
11. Suzuki, M., and Smith, J. M., *Chem. Eng. Sci.* **26**, 221 (1971).
12. Bennett, C. O., *AIChE J.* **13**, 890 (1967).
13. Matras, D., and Villermaux, J., *Chem. Eng. Sci.* **28**, 129 (1973).
14. Relya, D. L., and Perlmutter, D. A., *Ind. Eng. Chem. Process Des. Develop.* **7**, 261 (1968).
15. Balder, J. R., and Petersen, E. E., *J. Catal.* **11**, 195 (1968).
16. Balder, J. R., and Petersen, E. E., *Chem. Eng. Sci.* **23**, 1287 (1968).
17. Chambers, T. S., and Kistiakowsky, G. B., *J. Amer. Chem. Soc.* **56**, 399 (1934).
18. Schlag, E. W., and Rabinovitch, B. S., *J. Amer. Chem. Soc.* **82**, 5996 (1960).
19. Roberts, R. M., *J. Phys. Chem.* **63**, 1400 (1959).
20. Hall, W. K., Larson, J. G., and Gerberich, H. R., *J. Amer. Chem. Soc.* **85**, 3711 (1963).
21. Hall, W. K., Lutinski, F. E., and Gerberich, H. R., *J. Catal.* **3**, 512 (1964).
22. Hall, W. K., Larson, J. G., and Gerberich, H. R., *J. Amer. Chem. Soc.* **87**, 1880 (1965).

23. Hightower, J. W., and Hall, W. K., *J. Phys. Chem.* **72,** 4555 (1968).
24. Bartley, B. W., Habgood, H. W., and George, Z. M., *J. Phys. Chem.* **72,** 1689 (1968).
25. Basset, D. W., and Habgood, H. W., *J. Phys. Chem.* **64,** 769 (1960).
26. Habgood, H. W., and George, Z. M., "Catalytic Isomerization of Cyclopropane to Propylene over X and Y-Zeolites," Reprints of Soc. Chem. End., Conf. on Molecular Sieves, London, p. 130, 1967.
27. Kelly, J. F., "Parameter Estimation in Heterogeneous Catalysis." Ph.D. thesis, McGill University, Montreal, 1976.
28. Carberry, J. J., *Ind. Eng. Chem.* **56,** 39 (1964).
29. Roux, A. J., "Multicomponent Rates of Adsorption of Interactive $SO_2$ and $CO_2$ from Helium by Sodium Mordenite Molecular Sieve Adsorbents." M.S. thesis, Worcester Polytechnic Institute, Worcester, Mass., 1972.
30. Schobert, M. A., "Sorption and Isomerization of Cyclopropane on Synthetic Faujasite by Pulse Technique." Ph.D. thesis, Worcester Polytechnic Institute, Worcester, Mass., 1978.
31. Bosanquet, C. H., British T. A. Report, BR, 507 (1944).
32. Antonson, C. R., and Dranoff, J. S., *Chem. Eng. Prog. Symp. Ser.* **65,** 27 (1969).
33. Roberts, P. V., and York, R., *Ind. Eng. Chem. Process Des. Develop.* **6,** 516 (1967).
34. Sargent, R. W. H., and Whitford, C. J., *Advan. Chem. Ser.* **102,** 144 (1971).
35. Youngquist, G. R., Allen, J. L., and Eisenberg, J., *Ind. Eng. Chem. Prod. Res. Develop.* **10,** 308 (1971).
36. Mancel, C. P., "Diffusion of Gases in Zeolites by Gas Chromatography." Ph.D. thesis, Worcester Polytechnic Institute, Worcester, Mass., 1973.